One-Dimensional Analytical and Numerical Models of the Pulse-Tube Cooler

M.A. Etaati[1], R.M.M. Mattheij[1], A.S. Tijsseling[1], A.T.A.M. de Waele[2]

[1]Department of Mathematics and Computer Science
[2]Department of Applied Physics
Eindhoven University of Technology
Eindhoven, The Netherlands

ABSTRACT

Three one-dimensional models describing the fluid dynamics and thermodynamics in the tube section of a pulse-tube refrigerator have been developed: numerical, analytical and harmonic. The numerical model concerns a finite-difference scheme that is second-order accurate in space and time. The analytical model is exact and based on the method of characteristics. The harmonic model is approximate and assumes sinusoidal variations of all variables. Some typical results for a single-stage Stirling type pulse-tube refrigerator are presented.

INTRODUCTION

Pulse-tube refrigeration is based on a new concept that offers great advantages for further simplification of cooling technologies. In this paper we propose an accurate numerical model to simulate a Stirling type single-stage pulse tube refrigerator operating at high frequencies. The model describes the fluid dynamics and thermodynamics inside the tube.

A typical Stirling type pulse tube refrigerator is shown in Fig. 1. The refrigerator works by cyclic compression and expansion of gas, usually helium. The pressure oscillations in the system are generated by a piston. An after-cooler removes the heat of compression. The regenerator, which is made of a matrix of porous media having large heat capacity and large heat-exchanging surface, absorbs heat from the gas during compression and it returns heat to the gas during expansion. The cold heat exchanger is the coldest point of the system. Here the heat is removed from the gas. If there is a suitable phase relationship between the pressure variation and the oscillating gas flow in the tube, heat will be transported from the cold end to the warm end. The hot heat exchanger is kept at ambient temperature. Gas flows through the orifice to the reservoir, which is large compared to the pulse tube. Physical data for a typical single-inlet pulse tube are given in Table 1.

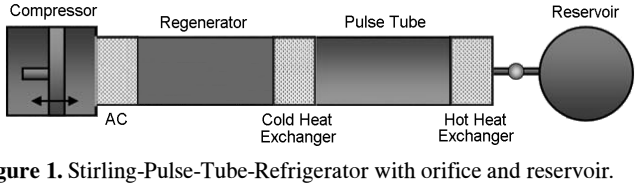

Figure 1. Stirling-Pulse-Tube-Refrigerator with orifice and reservoir.

Cryocoolers 14, edited by S.D. Miller and R.G. Ross, Jr.

Table 1. Physical data for a typical single-inlet pulse tube (values at 300 K).

Symbol	Definition	Value
f	frequency	20 Hz
ω	angular frequency	125.66 s^{-1}
$\bar{\rho}$	gas density	4.7 kg m^{-3}
$\bar{u}$	gas velocity	1.5 m s^{-1}
$\bar{\mu}$	viscosity	2.0×10^{-5} Pa s
$\bar{k}_g$	gas thermal conductivity	1.58×10^{-1} W m^{-1} K^{-1}
c_p	gas specific heat capacity	5.2×10^{3} J $kg^{-1}K^{-1}$
$\bar{p}$	pressure oscillation amplitude	5×10^{5} Pa
p_{av}	average pressure	3×10^{6} Pa
T_a	ambient temperature	300 K
R_m	specific gas constant	2.1×10^{3} J $kg^{-1}K^{-1}$
A_t	cross-sectional area of tube	2×10^{-3} m^2
C_{or}	flow conductance of the orifice	10^{-8} m^3 $Pa^{-1}s^{-1}$
L	length of tube	0.2m
T_H	hot end temperature	300K
T_C	cold end temperature	30K
V_b	buffer volume	5×10^{-3} m^3

MATHEMATICAL MODEL

We consider the one-dimensional region $0 < x < L$, where L is the length of the pulse tube. We assume that the fluid is Newtonian, the gas is ideal, and the flow is plug. We denote the density by $\rho(x,t)$, the velocity by $u(x,t)$, the temperature by $T(x,t)$, the pressure by $p(x,t)$, the dynamic viscosity by μ, the specific heat capacity of the gas at constant pressure by c_p, the thermal conductivity of the gas by k_g and the specific ideal gas constant by R_m. The equations for mass, momentum and energy conservation and the equation of state are:

$$\frac{\partial \rho}{\partial t} + \frac{\partial}{\partial x}(\rho u) = 0\,, \tag{1}$$

$$\rho\left(\frac{\partial u}{\partial t} + u\frac{\partial u}{\partial x}\right) = -\frac{\partial p}{\partial x} + \frac{4}{3}\frac{\partial}{\partial x}\left(\mu\frac{\partial u}{\partial x}\right), \tag{2}$$

$$\rho c_p\left(\frac{\partial T}{\partial t} + u\frac{\partial T}{\partial x}\right) = \frac{\partial p}{\partial t} + u\frac{\partial p}{\partial x} + \frac{\partial}{\partial x}\left(k_g\frac{\partial T}{\partial x}\right) + \frac{4}{3}\mu\left(\frac{\partial u}{\partial x}\right)^2, \tag{3}$$

$$p = \rho R_m T\,. \tag{4}$$

This system of equations is made non-dimensional and a low Mach-number approximation is applied yielding a uniform pressure variation in the tube.[1,2,3] The thermal conductivity, k_g, is assumed to be constant. The density is eliminated from the above set of equations and a time dependent (harmonic herein) pressure is the driving force of the system. The governing equations for the velocity and the temperature in terms of three auxiliary functions are

$$\frac{\partial u}{\partial x} = \varepsilon(t)\frac{\partial^2 T}{\partial x^2} + s_1(t), \tag{5}$$

$$\frac{\partial T}{\partial t} = \varepsilon(t)T\frac{\partial^2 T}{\partial x^2} - u\frac{\partial T}{\partial x} + s_2(t)T, \tag{6}$$

$$s_1(t) = -\frac{1}{(A + \bar{p}(t))\gamma}\frac{\mathrm{d}\bar{p}(t)}{\mathrm{d}t}, \tag{7}$$

$$s_2(t) = \frac{1}{A + \bar{p}(t)}\frac{\gamma - 1}{\gamma}\frac{\mathrm{d}\bar{p}(t)}{\mathrm{d}t}, \tag{8}$$

$$\varepsilon(t) = \frac{1}{B(A + \bar{p}(t))}\frac{1}{Pe}. \tag{9}$$

Table 2. Dimensionless parameters for a typical single-inlet pulse tube.

Symbol	Definition	Typical Value
Re	$\bar{\rho}\bar{u}^2/\bar{\mu}\omega$	4.2×10^3
Ma	$\bar{u}/(p_{av}/\bar{\rho})^{1/2}$	1.9×10^{-3}
M	$\bar{u}/(\bar{p}/\bar{\rho})^{1/2}$	4.6×10^{-3}
Pr	$c_p\bar{\mu}/\bar{k}_g$	0.66
Pe	RePr	2.772×10^3
$\mathcal{A}$	$p_0/\bar{p}$	6
$\mathcal{B}$	$\bar{p}/\bar{\rho}R_m T_a$	0.17
$\mathcal{C}$	$C_{or}\bar{p}/A_t\bar{u}$	1.67
$\mathcal{D}$	$C_{or}c_p\bar{p}/V_B c_v\omega$	$1/24\pi$
$\mathcal{E}$	$\bar{p}_b/\bar{p}$	6.048
γ	c_p/c_v	5/3

with A, B and Pe defined in Table 2. All variables are dimensionless and the pressure $\bar{p}$ is relative to an average system pressure. The temperature Equation (6) is a nonlinear convection-diffusion equation where the variable velocity *u(x,t)*, to be found from Eq. (5), determines the convection, and where $\varepsilon(t)$ *T(x,t)* is the variable diffusion coefficient. The coefficient $\varepsilon(t)$ is small as follows from dimensional analysis.[3] The temperature equation is then dominantly of a convective nature and therefore close to hyperbolic. To complete the system of equations for the tube, we define boundary and initial conditions. The boundary condition for Eq. (5) is provided by the velocity at the hot end through the orifice equation

$$u_H(t) = -C(\bar{p}(t) + A - \mathcal{E}\, p_b(t)) \tag{10}$$

Here $p_b(t)$ is the pressure in the buffer (reservoir) and $\bar{p}(t)$ is the dimensionless pressure variation in the tube. The coefficients A, C and ε are defined in Table 2, where $p_0 = p_{av}$. The buffer pressure is slightly changed (via ε) to prevent a net mass flow. The boundary conditions for Eq. (6) are velocity dependent: at the cold end, when the velocity is positive, the gas is coming out of the cold heat exchanger at constant low temperature, but when the velocity is negative, the gas is flowing back at the decreasing local temperature inside the tube. The same principle holds for the hot end. Therefore, we adopt the following boundary conditions for the temperature[3]:

$$\begin{cases} T(L,t) = T_H, & u(L,t) \le 0 \\ \dfrac{\partial T}{\partial x}(L,t) = [s_2(t)T(L,t) - \dfrac{\partial T}{\partial t}(L,t)]/u(L,t), & u(L,t) > 0 \end{cases} \tag{11}$$

$$\begin{cases} T(0,t) = T_C, & u(0,t) \ge 0 \\ \dfrac{\partial T}{\partial x}(0,t) = [s_2(t)T(0,t) - \dfrac{\partial T}{\partial t}(0,t)]/u(0,t), & u(0,t) < 0 \end{cases} \tag{12}$$

where T_H and T_C are the temperatures of the hot and cold heat exchangers, respectively. The hot end is usually at an ambient temperature around 300 K, and the cold end reaches temperatures in the range 30 K − 70 K. The initial condition for the temperature is taken linear according to

$$T(x,0) = T_C + (T_H - T_C)\frac{x}{L} \tag{13}$$

The linear initial condition for the velocity follows from the Eqs. (5) and (13).

NUMERICAL METHOD

To solve the problem numerically, the governing partial differential Equations (5)-(6) are discretized in space and time. We introduce computational grids corresponding to

$$x_j = jh, \quad j = 0,\ldots,N_x, \quad h = L/N_x,$$
$$t^n = n\tau^n, \quad n = 0,\ldots,N_t\,.$$

The velocity and temperature at the grid point (x_j, t^n) are denoted by u_j^n and T_j^n. The adaptive time step τ^n changes with u_j^n such that the CFL stability condition is always satisfied. We apply a second-order accurate scheme for the spatial discretization of the velocity Equation (5). For the temperature Equation (6) we apply a second-order scheme in space with central differences for the diffusion part and flux limiters for the convection part.[4] Moreover, a second-order time integration is used with the θ-method by taking $\theta = 0.5 + \tau^n$. The parameter values for the single-inlet pulse tube used in our simulations are given in Table 1. In our numerical experiments, we consider sinusoidal pressure variations of the form

$$p(t) = p_{av} - \overline{p}\sin(\omega t). \tag{14}$$

Thus, the driving pressure starts with expansion, before compression in the second half of each cycle.

ANALYTICAL SOLUTION

The governing Equations (1)-(4) are simplified by neglecting viscosity (μ=0), conductivity (k_g= 0), and inertia (the left side of Eq. (2)). The given absolute pressure is uniform (independent of x) and driving the system. An analytical solution can then be derived. The velocity is linear in x,

$$u(x,t) = u(x{=}0,t) - \frac{1}{\gamma p(t)}\frac{\mathrm{d}p(t)}{\mathrm{d}t}x, \tag{15}$$

where $u(\mathrm{x}{=}0,t)$ is defined by the boundary condition in Eq. (10), and the last term expresses gas compressibility. The gas displaces along characteristic paths in the distance-time plane for which $u{=}\mathrm{d}x/\mathrm{d}t$. Integration of Eq. (15) gives

$$x(t,x_0,t_0) = \int_{t_0}^{t} u(x{=}0,t)\left[\frac{p(\tau)}{p(t)}\right]^{\frac{1}{\gamma}}\mathrm{d}\tau + \left[\frac{p(t_0)}{p(t)}\right]^{\frac{1}{\gamma}}x_0, \tag{16}$$

where (x_0,t_0) is the characteristic path's start position at a boundary (at $t = 0$, $x = 0$, or $x = L$).

The temperature satisfies Poisson's law along a characteristic path,

$$T(t,x_0,t_0) = \left[\frac{p(t_0)}{p(t)}\right]^{1-\frac{1}{\gamma}} T(x_0,t_0), \tag{17}$$

with corresponding mass density

$$\rho(t,x_0,t_0) = \frac{p(t)}{R_m T(t,x_0,t_0)}. \tag{18}$$

RESULTS AND DISCUSSION

In Fig. 2 numerically calculated temperature profiles are shown at dimensionless times ωt=4π, 4.5π, 5π, and 5.5π, which correspond to different phases of the pressure cycle: 4π - start of expansion, 4.5π - minimum pressure (expansion), 5π - start of compression, and 5.5π - maximum pressure (compression). There is a very steep gradient in the temperature profile near the cold end of the tube, because the process started with an expansion. This gradient does not reach the (cold) boundary, and will therefore finally disappear due to thermal conduction. As can be seen from Fig. 3, there are no overshoots at the hot and cold ends as reported previously,[2,3] and these temperature plots fully agree with the harmonic approach of De Waele, et al.[5,6] In our numerical investigations, we try to demonstrate the beneficial effects of refining grids and using flux limiters, in particular with respect to maintaining the steep gradients in the temperature profile. Figure 4(a) shows that the finer the gird, the more accurate the results, as expected. Figure 4(b) shows how flux limiters, in this case Van Leer, improve the numerical results. Figure 5 shows the temperature history at the midpoint of the tube, calculated numerically and analytically. The small differences are probably due to slightly different buffer pressures used in the simulations.

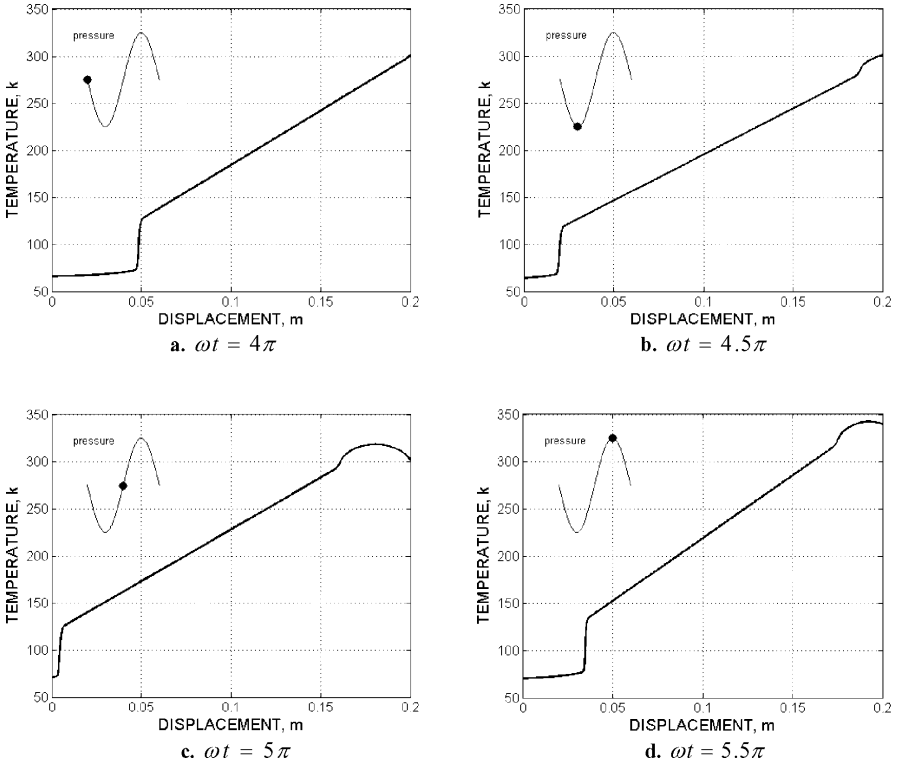

Figure 2. Temperature profiles at four phases of one pressure cycle.

CONCLUSION

A one-dimensional numerical model has been developed for simulating oscillating gas flow in the tube section of a pulse-tube refrigerator. The model is second-order accurate in both space and time. The conservation laws and the ideal gas law have been transformed into two equations governing velocity and temperature. The behavior of temperature and velocity in the pulse tube, especially near the cold and hot ends, has been numerically investigated. DC flow is avoided by a buffer pressure slightly higher than the average pressure in the pulse tube. Undesired temperature overshoots are avoided by starting the process with an expansion. The efficiency of flux limiters has been demonstrated. An analytical solution has been used to successfully verify the numerical results.

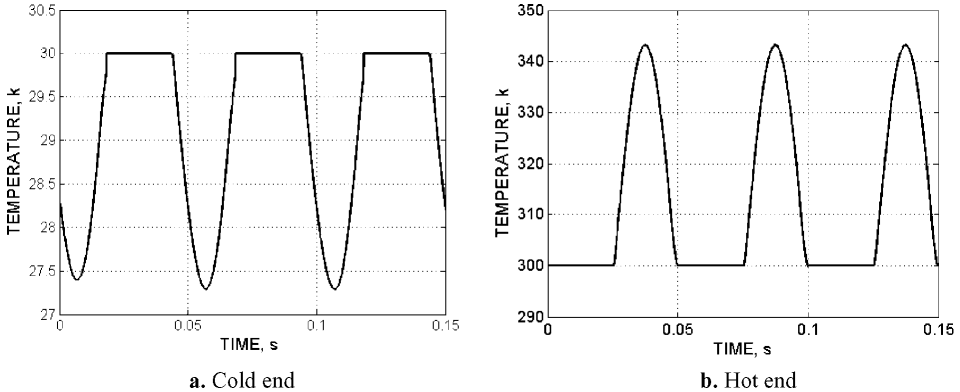

Figure 3. Temperature at the cold and hot ends for three cycles.

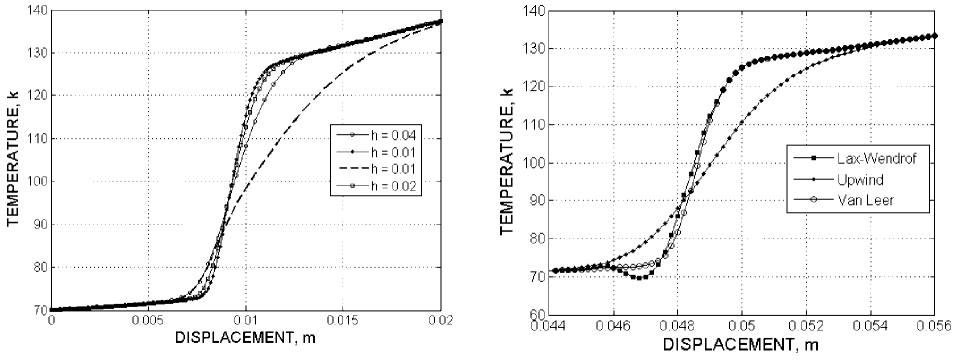

a. Different grid sizes **b.** Different numerical methods

Figure 4. Temperature profiles for different grid sizes and different numerical methods.

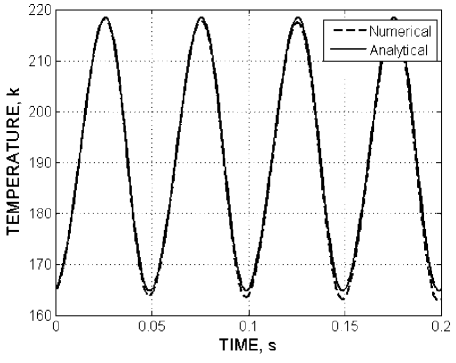

Figure 5. Temperature for four cycles in the middle of the tube.

ACKNOWLEDGMENT

This project is financed by STW (Dutch Technology Foundation), project number: ETF. 6595.

REFERENCES

1. Smith, W.R., "One-dimensional Models for Heat and Mass Transfer in Pulse Tube Refrigerators," *Cryogenics*, 41 (2001), pp. 573-582.

2. Lyulina, I.A., Mattheij, R.M.M., Tijsseling, A.S., De Waele, A.T.A.M., "Numerical simulation of pulse-tube refrigerators," *International Journal of Nonlinear Sciences and Numerical Simulation*, 5(2004), pp. 79-88. Corrigenda: 5 (2004), p. 287.

3. Lyulina, I.A., *Numerical Simulation of Pulse-Tube Refrigerators*, PhD Thesis, Dept. of Mathematics and Computer Science, Eindhoven University of Technology, Eindhoven, The Netherlands (2005).

4. Mattheij, R.M.M., Rienstra, S.W., Boonkkamp, J.H.M. ten Thije, *Partial Differential Equations, Modelling, Analysis, Computing*, SIAM Press, Philadelphia (2005).

5. De Waele, A.T.A.M., Steijaert, P.P., Gijzen, J., "Thermodynamical Aspects of Pulse Tubes," *Cryogenics*, 37 (1997), pp. 313-324.

6. De Waele, A.T.A.M., Steijaert, P.P., Koning, J.J., "Thermodynamical Aspects of Pulse Tubes II," *Cryogenics*, 38 (1998), pp. 329-335.